Proceedings of the 17th International Heat Transfer Conference, IHTC-17

14 – 18 August 2023, Cape Town, South Africa

IHTC-17 | ID: 309

THE DISPERSION OF A HIGH TEMPERATURE AIR JET IN A BLUFF BODY WAKE

Isaac Stephens, Ieuan Owen, Mark White

The University of Liverpool, Liverpool, L69 7ZX, UK

ABSTRACT

This paper describes an experimental study in which a hot air jet is discharged from a 25 mm nozzle at the centre of the top surface of a cuboid placed on the floor of a wind tunnel. The cuboid has a cross section of 0.2 m x 0.2 m and a length of 0.4 m. A 12.7 μm fine-wire thermocouple has been used to measure the unsteady temperatures within the jet plume as it is swept downstream by the cross-flow. Dimensional analysis indicates that the trajectory and temperatures within the plume are momentum-dominated and are governed by the jet to cross-flow momentum flux ratio. Three different jet temperatures and velocities were therefore selected to give a constant momentum flux ratio and the similarity of the normalised temperature profiles downstream of the jet nozzle confirmed the dimensional analysis. The study being reported is part of a larger project to investigate the dispersion of hot engine exhaust gases from a ship's engines, and how they interact with the ship's helicopter. The experimental results from the generic bluff-body geometry of a cuboid will be compared with the results from an unsteady Computational Fluid Dynamics (CFD) analysis to provide confidence in the CFD methodology that will then be applied to the full-scale ship. The temperature measurements presented in the paper have been compared with a preliminary steady-state CFD analysis with encouraging results.

KEY WORDS: Wind tunnel, Bluff body, Heated jet, Cross-flow, Ship, Helicopter.

1. INTRODUCTION

The motivation for the experimental study being reported in this paper is to gain a better understanding of how the hot exhaust gases from a ship's gas turbine engine are dispersed, and how they affect the operation of the ship's helicopter. The scenario is illustrated in Fig.1, which has been extracted from a previous study by Scott et al. [1]. The image shows the results of an unsteady Computational Fluid Dynamics (CFD) analysis of the dispersion of a combat ship's engine exhausts in a 40 knots headwind. The top image shows isosurfaces of mean temperature (1, 2 and 5°C), while the bottom image shows isosurfaces of instantaneous temperature. Looking closely at the top image, the exhaust gas can be seen emerging from the gas turbine uptake, amidship (marked GT); the jet is quickly deflected by the wind and passes over the flight deck at the stern of the ship. Also shown in the image is the exhaust flow from the ship's Diesel generators (DG), which is also deflected towards the flight deck. In [1] the exhaust gas was considered to have the properties of air and was discharged from the gas turbine at 131 kg/s and 565°C; the Diesel generator flow rate and temperature was 5.5 kg/s and 400°C. During a normal landing procedure, prior to touchdown, the helicopter would hover above the deck at the lower position shown in the image; the higher position represents where the helicopter might hover with an underslung load. It can clearly be seen that the helicopter will be immersed in the exhaust plume, and while the temperatures do not seem high, the maximum air temperature rise recommended for a helicopter operating to an offshore oil/gas platform is 2°C, averaged over 3 seconds [2]. The

*Corresponding Author: sgisteph@liverpool.ac.uk

instantaneous temperatures in the lower image in Fig. 1 show that the dispersion of the exhaust gases is more chaotic than suggested by the time-averaged temperatures. The fluctuations in the air temperature are also important as they can adversely affect the control system of the helicopter's engines [2]; therefore, a meaningful CFD analysis needs to be unsteady.

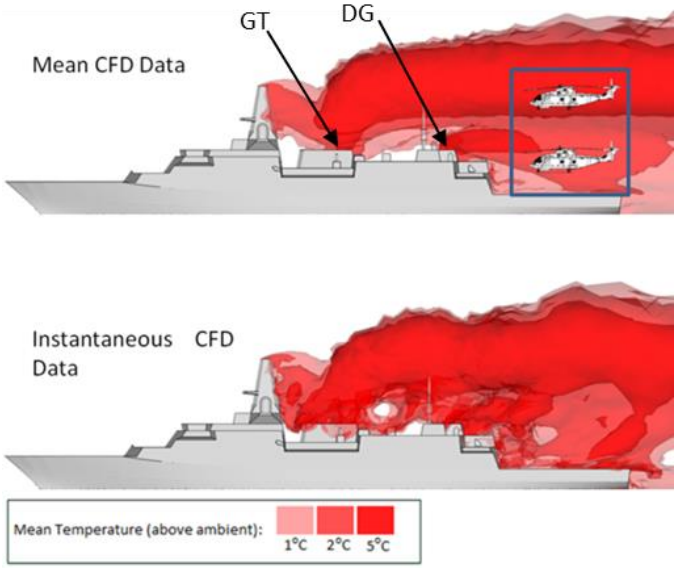

Fig. 1 CFD analysis of the dispersion of a ship's engine exhaust gas [1]

As in all CFD analyses, it is important to validate the computational results through comparison with experimental data. For the relatively complex scenario described above, there is no suitable experimental data; hence the study being reported herein. What has been studied in the past is the discharge of a heated jet from a flat surface into a steady cross-flow, which is different from discharging a heated jet into a cross-flow formed by the wake of a bluff body, where the turbulent flow will significantly affect the mixing processes, and the dispersion and cooling of the jet.

Previous experimental studies of jets in cross-flow [3]–[6] have placed a heated jet flush with the floor of a wind tunnel, or upon a raised floor to eliminate the incoming boundary layer. In the current study, the heated jet is discharged from the upper face of a cuboid placed in a wind tunnel, acting as a bluff body and thereby providing experimental data for a generic geometry. The trajectory of the plume from the perpendicular jet can be characterised through a dimensional analysis where the trajectory, s, of the jet is a function of the velocity, density and dynamic viscosity of the jet and the cross-flow, as well as the geometry, here characterised by the diameter of the pipe discharging the jet.

$$s = f\left(U_0, U_j, \rho_0, \rho_j, \mu_0, \mu_j, g, D_j\right) \tag{1}$$

Such an analysis, assuming the dynamic scaling is insensitive to the Reynolds numbers of both the jet and the cross-flow, shows that the dimensionless temperature has a functional relationship with the momentum flux ratio of the jet and the cross-flow, and the Richardson number, which accounts for the buoyancy forces, i.e.

$$\left\{\frac{\mathrm{T}-\mathrm{T}_0}{\mathrm{T}_j-\mathrm{T}_0}\right\} = f\left\{\frac{\rho_j \mathrm{U}_j^2}{\rho_0 \mathrm{U}_0^2}, \frac{g L}{U_0^2}\frac{\left(\rho_0-\rho_j\right)}{\rho_0}\right\} \tag{2}$$

However, in highly turbulent flow the mixing process is momentum-dominated and the weaker buoyancy force has little effect. Therefore, the jet trajectory and the mixing processes are a function of the momentum flux ratio. This assertion was tested in the present study by measuring the temperature profiles in the jet plume for a constant momentum flux ratio but with three different combinations of jet and cross-flow velocity and temperature.

2. METHODOLOGY

An experiment was conducted in which a hot air jet was discharged from a 25 mm internal diameter nozzle located at the centre of the top surface of a cuboid 0.20 m in width and height, and 0.40 m length in the streamwise direction. The wind tunnel has a rectangular working section measuring 1.22 m across and 0.61 m high, shown schematically in Fig. 2. The hot jet is discharged vertically upwards while the horizontal cross-flow is delivered by a 2-stage fan driven by a 20 horsepower D.C brushless motor. Following the fan, the wind tunnel opens into a 2.5 m^2 settling chamber, where the flow slows and passes through a perforated steel plate, and a coarse and a fine honeycomb mesh, before being accelerated via a rectangular contraction to the working section.

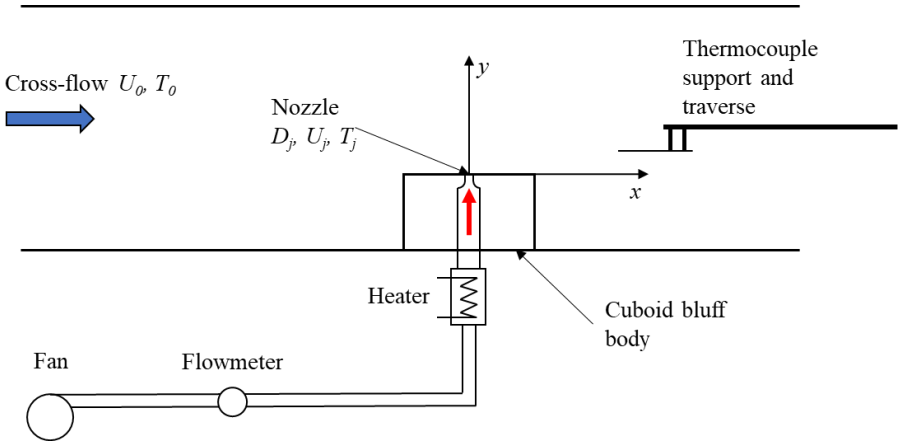

Fig. 2 Wind tunnel schematic

The air supply to the jet was provided by a small, controllable, centrifugal blower and the air mass flow rate was measured by a vortex-shedding flowmeter before entering a heating chamber with controllable electric heating elements. The heated air then entered a radiused contraction section into the 25 mm diameter pipe which had a 25 mm parallel section, thereby forming a short nozzle and a jet with a uniform velocity profile. A thermocouple was placed between the heating chamber and the nozzle to monitor the air temperature and to control the heater.

The initial stage of the experiment used smoke flow visualisation to select a set of flow/temperature combinations for the jet and the cross-flow which produced an energetic flow in which the jet did not get too close to the roof of the wind tunnel; the flow visualisation was also used to identify where temperature measurements were to be made. All the temperatures reported in this paper were measured on a vertical plane through the longitudinal centreline of the jet (and the cuboid). Table 1 shows the three sets of conditions that were used in the experiment, each produce a momentum flux ratio of about 11.

Table 1 Experimental conditions

	Jet		Cross-flow	
	Velocity, U_j m/s	Temp., T_j °C	Velocity, U_0 m/s	Temp., T_0 °C
Run 1	15.1	125	3.9	16.7
Run 2	12.5	52	3.5	12.5
Run 3	15.8	144	3.9	13.3

As mentioned in the Introduction, both the mean temperature in the jet and the unsteady fluctuations are important and therefore a fast-response thermocouple was required. The temperatures were measured using a 12.7 μm diameter Medtherm fine-wire type-K thermocouple [7] attached to a 3-dimensional traverse system. The signal produced by the thermocouple was passed through an amplifier, before reaching a 14-bit data acquisition system. According to Carbon et al. [8], the response of the thermocouple can be estimated using a heat balance analysis to form an equation for the temperature, T, of the thermocouple junction τ seconds after a step change in air temperature from T_i to T_a :

$$(T_i - T) = (T_i - T_a)\left(1 - e^{-\frac{\tau}{\beta}}\right) \tag{3}$$

Where:

$$\beta = \frac{\rho_t D_t c_t}{4h} \tag{4}$$

The value for heat transfer coefficient, h, is obtained from a correlation provided by McAdams [9]:

$$\frac{hD_t}{k_0} = 0.32 + 0.43\left(\frac{D_t U \rho_0}{\mu_0}\right)^{0.52} \tag{5}$$

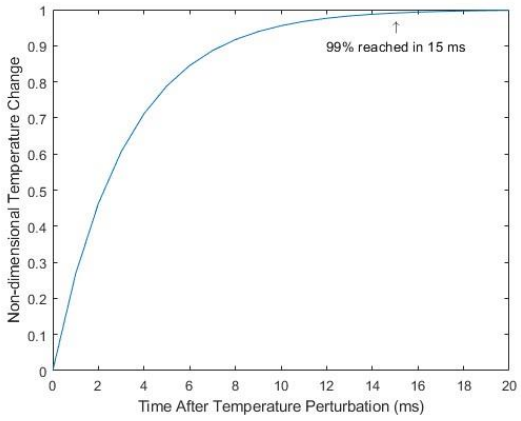

Fig. 3 Thermocouple response time

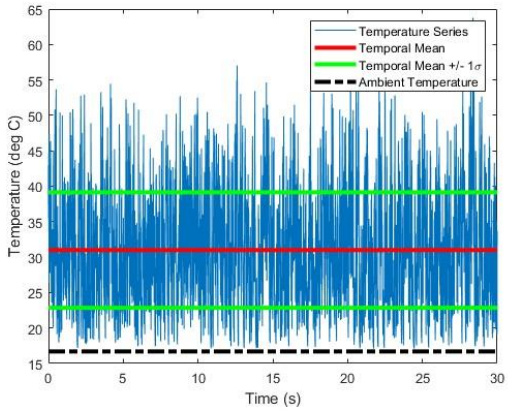

Fig. 4 Thermocouple output, *x/R* = 2, *y/R* = 11

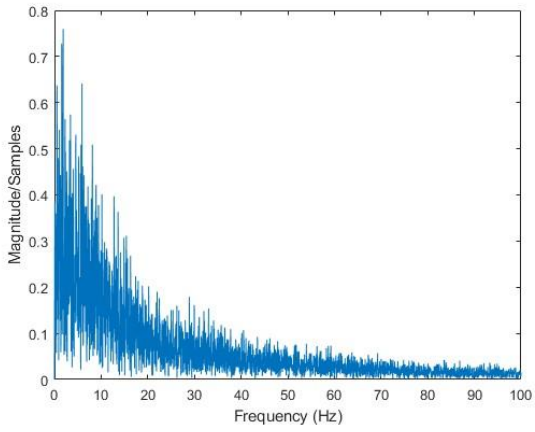

Fig. 5 Fast Fourier transform of unsteady thermocouple output, *x/R* = 2, *y/R* = 11

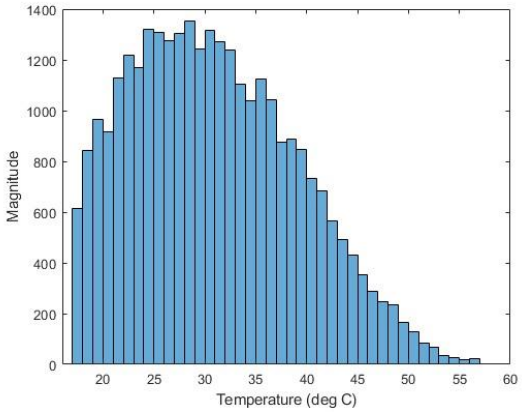

Fig. 6 Probability distribution of unsteady thermocouple output, *x/R* = 2, *y/R* = 11

Inserting the appropriate property values for the thermocouple material and the air leads to the graph in Fig. 3, which shows that the thermocouple will reach 95% of its reading in 12 ms, and 99% of its reading in 15 ms. A preliminary experiment was therefore conducted to investigate the unsteady temperatures and their frequency content to assess the suitability of the fine-wire thermocouple. Figure 4 shows the unsteady temperature measured by the thermocouple at a location where the highest fluctuations occurred (a distance of two pipe radii downstream of the pipe centreline, and a height above the jet outlet of 11 radii). Also shown on this graph are ±1 standard deviation. Figure 5 shows a fast Fourier transform of the data in Fig. 4, where it can be seen that the frequency content of the unsteady temperature is mostly below 50 Hz, or 20 ms, and so the thermocouple is reasonably capable of following the unsteady temperature fluctuations. It should be noted, however, that the probability distribution of the unsteady temperature is a truncated normal distribution, as shown in Fig. 5. The reason for this is that the temperature values below the mean are limited to whatever the ambient temperature is, as indicated in Fig. 4. While it is still appropriate to characterise a non-gaussian distribution by the mean and standard deviation, the usual assumptions related to a normal distribution do not apply.

3. RESULTS

3.1 Profiles of Mean Temperature

Having determined the area occupied by the jet plume and the frequency response of the thermocouple, a series of vertical traverses were made downstream of the jet exit, in the vertical plane through the centreline of the jet. Unsteady temperature data were recorded for Run 1 settings (Table 1) at 7 streamwise stations, at distances of 2, 5, 10, 16, 24, 30, and 39 nozzle radii from the axis of the jet nozzle, spanning vertically from 1cm above the cuboid, to 25 nozzle radii above the cuboid, in increments of 1 nozzle radius. At each location, a sampling frequency of 1,000Hz was used over a period of 30 seconds. The ambient cross-flow had a mean velocity of 3.9m/s, measured using a 2.5Hz pitot-static tube located upstream of the cuboid, at an ambient temperature of 16.7°C. The heated jet had a temperature of 125°C and a mean velocity of 15.1m/s.

The resulting normalised mean temperature profiles are shown in Fig. 7. The first thing to notice is how quickly the hot jet has cooled, and this is further illustrated in Fig. 8 where it can be seen that the maximum temperature in the jet has fallen from its initial vale of 125°C to about 55°C by the first measurement location. This steep reduction in the temperature in the jet is due to the highly energetic mixing processes and is consistent with the temperature values shown in Fig. 1 where the original gas turbine exhaust temperature of 565°C was predicted to fall to an average temperature of about 5°C above ambient by the time the plume reached the flight deck.

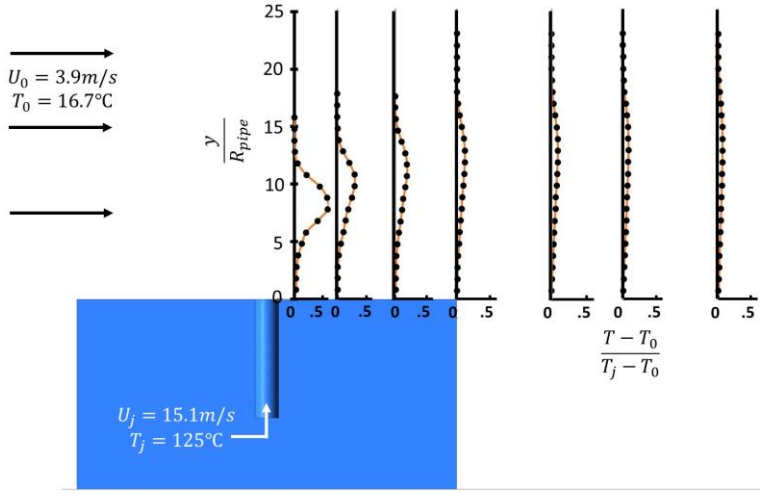

Fig. 7 Profiles of normalised temperature profiles downstream of the jet nozzle

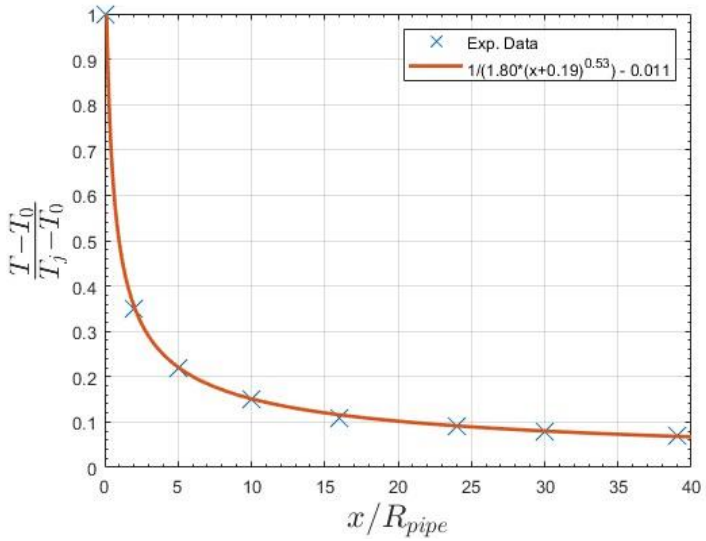

Fig. 8 Decay of maximum jet temperature downstream of jet nozzle.

3.2 Profiles of Temperature Fluctuations

As discussed in the Introduction, it is also important to include the temperature fluctuations when using CFD to predict the air temperatures in which a ship's helicopter will operate. The fluctuations in the experiment have been characterized by the standard deviation, and these have been normalized by the difference between the initial jet temperature and the ambient temperature, as shown in Fig. 9.

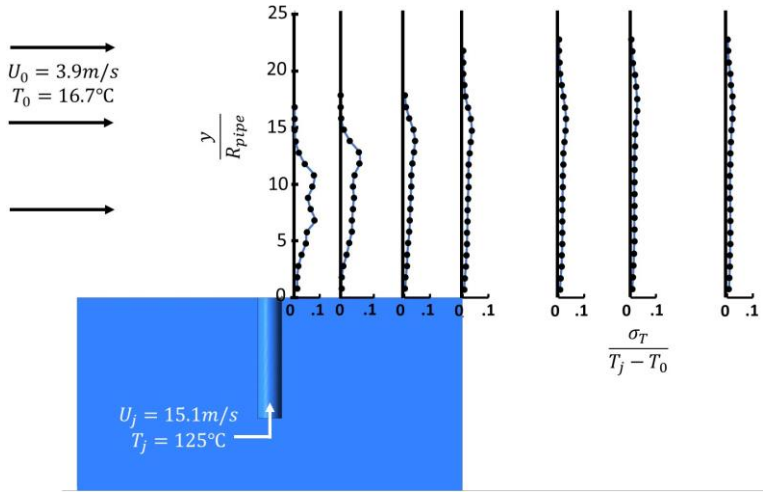

Fig. 9 Profiles of normalized standard deviation of temperature fluctuations

It can be seen in Fig. 9 that the first profile has a double-peak in the temperature fluctuations; this is a characteristic of a heated jet discharging into a still ambient environment where a turbulent shear layer forms at the outer surface of the jet [10]. However, it can be seen that the double peak has disappeared by the second measurement location, indicating that the initial core of the jet has already been mixed with the cross-flow. As was seen in Fig. 7, the temperature of the jet plume quickly reduces, so the magnitude of the difference between the fluctuating temperatures in the jet and the ambient temperature also diminish quickly, as seen in Fig. 9.

3.3 Jet dispersion at constant momentum flux ratio

Equation (2), which emerged from a dimensional analysis of a hot jet mixing with a cooler cross-flow, shows the dimensionless temperatures to be dependent on the jet to cross-flow momentum flux ratio and the Richardson number. The rapid cooling of the jet, illustrated in Figs. 7 to 9, are indicative of a strongly momentum-dominated mixing between the jet and the cross-flow and therefore it was postulated that the jet dispersion and dimensionless temperature distribution are a function only of the momentum flux ratio, and that the buoyancy dependency is secondary. This hypothesis was tested by repeating the experiment with two additional conditions, shown earlier in Table 1 as Runs 2 and 3.

The comparisons for the three cases are made in Figs. 10 and 11, for profiles of mean and standard deviation of the jet temperatures at three downstream locations. The data for the three cases do not collapse perfectly at the first location, but here the gradients of velocity and temperature will be very steep, and so the validity of the dimensional analysis, which applies to representative parameters of the flow, is probably being stretched. However, as can be seen at the other two locations, the profiles have collapsed very well, confirming that the temperature distribution and trajectory of the jet is governed by the jet to cross-flow momentum flux ratio.

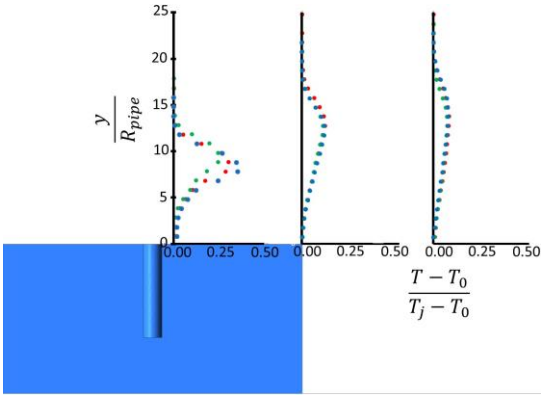

Fig. 10 Profiles of normalized temperature for different flow conditions and constant momentum flux ratio
●Run 1, ●Run 2, ●Run 3.

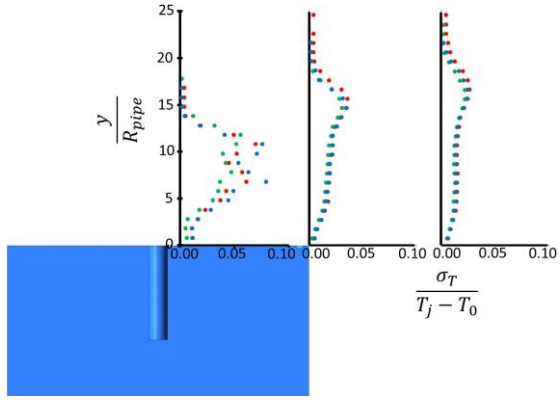

Fig. 11 Profiles of normalized standard deviation of temperature fluctuations for different flow conditions and constant momentum flux ratio
●Run 1, ●Run 2, ●Run 3.

3.4 Reynolds-Averaged Navier-Stokes CFD simulation

As discussed in the Introduction section, the purpose of this experimental study was to provide measured data for comparison with CFD predictions of a hot jet mixing in turbulent cross flow over a generic bluff body. The aim in the near future is to compare the experiment with unsteady CFD, using Delayed-Detached Eddy Simulation (DDES), so that the temperature fluctuations can be obtained along with the mean temperatures within the jet plume. In preparation for the unsteady analysis, a preliminary study has been carried out where the mean temperature data from Run 1, Fig. 7, was compared with the results of a time-averaged CFD simulation of the plume's trajectory. The working section of the wind tunnel was modelled, placing the inlet 6.25 box lengths ahead of the box, and the outlet 1.5 lengths behind the box. The pipe from which the perpendicular jet escapes is extruded 10 pipe radii into the box, corresponding to the end of the contraction section in the pipe where a uniform flow is expected to enter into the domain. Matching the experimental conditions, the cross-flow velocity is set as 3.9 m/s with a temperature of 16.7 ℃, and the perpendicular jet was given a mass-flow rate of 6.6 g/s, at a temperature of 125 ℃. Both inlets were assigned uniform velocity profiles.

From the injection of the cross-flow to a distance of 1 box height upstream of the box, a coarse mesh is used, where velocity gradients are expected to be small. Approaching the box and continuing until the outlet of the domain, a much finer resolution is used to capture the mixing between the plume and the cross-flow, as well as the flow features around the box. The sizing used in the fine mesh region was selected as a result of a grid-dependence study, where the mesh size ranged from 0.4 to 4 pipe radii. The final unstructured mesh consists of elements measured 0.5 pipe radii in the near-block region, and 1.8 pipe radii in the upstream zone. Blanketing the walls of the domain, 22 prism layers ensure the value of y^+ remains below 1.0 in the downstream region of the domain. As a result, the domain consists of 26 million unstructured tetrahedral elements.

ANSYS Fluent was employed to solve the steady, compressible Reynolds-Averaged Navier-Stokes equations, closed using the Shear Stress Transport (SST) k-omega turbulence model [11]. The SST model blends the strengths of the k-epsilon turbulence model in the free-stream with the near-wall flow modelling of the k-omega model. Initially, the governing equations are solved using first-order discretization to provide a stable solution, before switching to second-order discretization for improved accuracy.

In Fig. 12, the profiles of temperature above ambient at each stream-wise station is plotted from both the experimental data and the simulation data, overlaid on contours of temperature above ambient. The agreement at the first measurement location, close to the emerging jet, is not perfect; this observation, taken together with the differences in the normalized temperatures shown earlier in Figs. 10 and 11 suggest the mixing processes close to the jet source are a challenge for both the CFD and the dimensional analysis, due to the steep gradients that exist in both the velocity and temperature fields. However, with increasing distance from the jet outlet, the agreement between the temperature profiles of the experiment and the simulation improve.

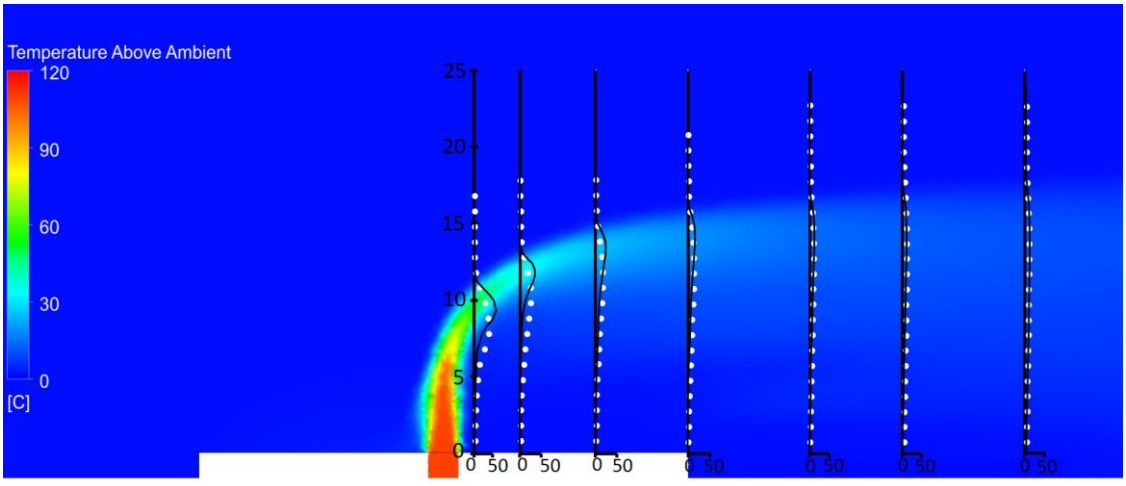

Fig. 12 Comparison of experimental temperatures (white dots) with CFD temperature profiles, overlaid on temperature contours

4. CONCLUDING COMMENTS

This paper has described an experiment in which a hot air jet was discharged from the top of a bluff body into an ambient cross-flow. The purpose was to provide experimental data for a generic geometry from which the unsteady temperatures within the jet plume could be compared with CFD predictions.

The study has shown how the mixing between the perpendicular hot jet and the ambient cross-flow results in a rapid decay of temperature within a short distance from the jet outlet. At each stream-wise station, temperature decays greatest from the top of the jet, where it is more exposed to the ambient cross-flow. Similar patterns have been observed from jets emerging from a flat surface into a cross-flow [12].

A dimensional analysis of the jet mixing and dispersion has indicated that the trajectory of the jet and the temperatures within it are governed by the momentum flux ratio between the jet and the cross-flow. Altering the density and velocity ratios, while maintaining the momentum flux ratio, had little effect on the normalized temperature profile in the plume. Similarly, the profiles of temperature standard deviation were found to be independent of density and velocity ratios. The negligible impact of density and velocity ratios on the plume has also been found in experiments with perpendicular jets from flat surfaces [13]. From a distance of 16 pipe radii, until the end of the experimental domain, the plume's core remains at a fixed height, which supports the assumption that the flow is momentum-dominated, and the effects of buoyancy are insignificant in the current experimental domain.

A comparison of the experimental results with a steady-state CFD analysis shows encouraging agreement; the intention is to extend the CFD analysis by applying DDES, a time-accurate CFD method which resolves turbulent eddies as small as the grid scale [14]. Further CFD analysis and velocity measurements within the jet will be used to reinforce the confidence in the CFD method before it is used to predict the dispersion of engine exhaust gas flow over a full-scale ship.

NOMENCLATURE

c_t	specific heat of thermocouple material	[J/kgK]
D_j	diameter of perpendicular jet	[m]
D_t	diameter of thermocouple wire	[m]
g	acceleration due to gravity	[m/s^2]
h	coefficient of heat transfer	[]
k_0	thermal conductivity of air	[W/mK]
s	jet trajectory	[]
T	temperature indicated by thermocouple τ seconds after change occurs	[K]
T_0	ambient temperature	[K]
T_a	temperature of air stream after temperature change occurs	[K]
T_i	initial temperature as indicated by thermocouple before temperature change occurs	[K]
T_j	temperature of the perpendicular jet	[K]
U	flow velocity	[m/s]
U_0	cross-flow velocity	[m/s]
U_j	jet velocity	[m/s]
x	stream-wise distance	[m]
y	vertical distance	[m]
μ_0	cross-flow air dynamic viscosity	[kg/ms]
μ_j	jet flow dynamic viscosity	[kg/ms]
ρ_0	cross-flow air density	[kg/m^3]
ρ_j	jet air density	[kg/m^3]
ρ_t	density of thermocouple material	[kg/m^3]
τ	time elapsed after temperature change occurs	[s]

REFERENCES

[1] P. Scott, M. White, and I. Owen, “Unsteady CFD Modelling of Ship Engine Exhaust Gases and Over-Deck Air Temperatures, and the Implications for Maritime Helicopter Operations,” in *AHS 71st Annual Forum*, May 2015, pp. 1–9.

[2] Civil Aviation Authority, “CAP 437: Standards for Offshore Helicopter Landing Areas,” 2021. [Online]. Available: www.caa.co.uk/CAP437

[3] E. E. Callaghan and D. T. Bowden, “Investigation Of Flow Coefficient Of Circular, Square, And Elliptical Orifices At High Pressure Ratios,” Washington, 1949.

[4] E. E. Callaghan and R. S. Ruggeri, “Investigation of the Penetration of an Air Jet Directed Perpendicular to an Air Stream,” Washington, 1948.

[5] E. E. Callaghan and R. S. Ruggeri, “A General, Correlation of Temperature Profiles Downstream of a Heated-Air Jet Directed Perpendicularly To an Air Stream,” NACA, 1951. [Online]. Available: http://hdl.handle.net/2060/19810068722

[6] R. S. Ruggeri, E. E. Callaghan, and D. T. Bowden, “Penetration of Air Jets Issuing From Circular, Square, and Elliptical Orifices Directed Perpendicularly to an Air Stream,” 1950.

[7] Medtherm Corporation, “Fine Wire Thermocouple Probes for measuring Transient Gas Temperatures,” *https://kt-messtechnik.de/downloads/TCFW_Brochure_B112.pdf*, Dec. 28, 2022.

[8] M. W. Carbon, H. J. Kutsch, and G. A. Hawkins, “The Response of Thermocouples to Rapid Gas-Temperature Changes,” in *ASME*, 1950, pp. 655–657.

[9] W. H. Mcadams, *Heat Transmission*, 2nd ed. New York: Mcgraw-Hill Book Company, 1942.

[10] J. Bashir and M. S. Uberoi, “Experiments on turbulent structure and heat transfer in a two-dimensional jet,” *Physics of Fluids*, vol. 18, no. 4, pp. 405–410, 1975, doi: 10.1063/1.861164.

[11] F. R. Menter, ‘Two-equation eddy-viscosity turbulence models for engineering applications’, *AIAA Journal*, vol. 32, no. 8, pp. 1598–1605, 1994, doi: 10.2514/3.12149.

[12] J. W. Ramsey and R. J. Goldstein, “Interaction of a Heated Jet With a Deflecting Stream,” *ASME Pap*, no. 71, 1971.

[13] Y. Kamotani and I. Greber, “Experiments on a Turbulent Jet in a Cross Flow,” *AIAA Journal*, vol. 10, no. 11, pp. 1425–1429, Nov. 1972, doi: 10.2514/3.50386.

[14] P. R. Spalart, W.-H. Jou, M. Strelets, and S. R. Allmaras, “Comments on the Feasibility of LES for Wings, and on a Hybrid RANS/LES Approach,” in *Proceedings of first AFOSR international conference on DNS/LES*, 1997.